frontiers | Frontiers in Earth Science

TYPE Original Research
PUBLISHED 29 September 2025
DOI 10.3389/feart.2025.1667992

OPEN ACCESS

EDITED BY
Gang Rao,
Southwest Petroleum University, China

REVIEWED BY
Daoyang Yuan,
Lanzhou University, China
Bing Yan,
Hohai University, China

*CORRESPONDENCE
Lichun Chen,
glutclc@glut.edu.cn

RECEIVED 17 July 2025
ACCEPTED 15 September 2025
PUBLISHED 29 September 2025

CITATION
Han M, Wang S, Li Y, Chen L, Li X, Wang D and Zeng X (2025) Late quaternary activity characteristics of the Quzika-Jitang segment along the Lancangjiang fault zone, eastern Tibetan Plateau.
Front. Earth Sci. 13:1667992.
doi: 10.3389/feart.2025.1667992

Late quaternary activity characteristics of the Quzika-Jitang segment along the Lancangjiang fault zone, eastern Tibetan Plateau

Mingming Han[1,2], Shiyuan Wang[3], Yanbao Li[2], Lichun Chen[4]*, Xuemei Li[5], Dongbing Wang[1] and Xiaowen Zeng[1]

[1]Chengdu Center, China Geological Survey (Geosciences Innovation Center of Southwest China), Chengdu, China, [2]Institute of Geology, China Earthquake Administration, Beijing, China, [3]Sichuan Earthquake Agency, Chengdu, China, [4]College of Earth Sciences, Guilin University of Technology, Guilin, China, [5]Tuojiang River Basin High-Quality Development Research Center, Neijiang Normal University, Neijiang, China

The Lancangjiang fault zone (LCJFZ) is a major crustal-scale fault system that traverses the Sichuan-Tibet traffic corridor. Determining its late Quaternary activity is thus crucial for assessing seismic hazards and guiding the planning of this critical infrastructure. However, there is no clear evidence as to whether the fault zone has been active since the late Quaternary. Although recent studies have suggested that the Lancangjiang fault (LCJF), a main branch of the LCJFZ, offsets Holocene sediments near the Jitang and Quzika sites and is therefore active, the supporting evidence remains inconclusive. In this paper, we carried out detailed field investigation along the Quzika-Jitang segment, building on previous work. Combined with radiocarbon dating, we reassessed the late Quaternary activity of the LCJF. Our new results reveal that the nearly SN-trending segment of the LCJF (F1) shows no sign of late Quaternary activity. In contrast, the NE-trending branch fault of the LCJF (F2), located near Quzika Township, has faulted the late Quaternary strata and may exhibit Holocene activity. Further analysis suggests that the LCJFZ is no longer the main structure regulating regional tectonic deformation. Instead, secondary strike-slip faults, such as fault F2 and the Yangda-Yaxu fault (YYF), cut through or intersect the LCJFZ, and exhibit obvious late Quaternary activity. Thus, we speculate that the NE-trending F2 and WNW-trending YYF are both probably the most active structures around the LCJFZ today. These observations indicate that the main structures absorbing and regulating regional strain energy have changed from nearly SN-trending LCJFZ to several secondary WNW- and NE-trending faults, which means that tectonic transformation and fault neogenesis have occurred around the LCJFZ.

KEYWORDS

Langcangjiang fault zone, fault activity, secondary fault, tectonic transformation and fault neogenesis, three parallel Rivers region

1 Introduction

The Sichuan-Tibet traffic corridor (STTC) connects the Sichuan Basin and the Tibetan Plateau from east to west (Lu and Cai, 2019; Cui et al., 2022). It serves as an important strategic and economic artery in southwestern China (Pan et al., 2020; Pei et al., 2023). The impact effects of northward subduction of the Indian Plate and southeastward extrusion of the Tibetan Plateau result in intense tectonic movement and the development of numerous major fault systems along the corridor, which further leads to frequent geological hazards in this region (Yin and Harrison, 2000; Tapponnier et al., 2001; Taylor et al., 2003; Li et al., 2020; Li et al., 2021; Zhang D. et al., 2022). These hazards, especially those related to fault activity, can strongly interfere with the transportation facilities within the corridor. Therefore, it is extremely important to investigate the current activity characteristics of faults in this area.

The Nujiang, Lancangjiang and Jinshajiang fault zones (abbreviated as NJFZ, LCJFZ, and JSJFZ, respectively) are three major, nearly SN-trending fault systems in the Hengduan Mountains Region that traverse the Sichuan-Tibet traffic corridor (Figure 1; Yin and Harrison, 2000; Taylor et al., 2003; Guynn et al., 2006; Ren et al., 2022; Li et al., 2023). It is therefore critical to characterize the activity of these three fault systems. However, owing to strong erosion, inaccessibility, and a harsh climate in the high mountain and canyon areas, geomorphic evidence is poorly preserved. Consequently, previous studies have mainly targeted the JSJFZ at the western boundary of the Sichuan-Yunnan block and the NJFZ with records of $M \geq 7$ earthquakes (Xia and Zhu, 2020; Han et al., 2022a; Zhong et al., 2022; Liang et al., 2025). In contrast, the LCJFZ has received even less attention due to a lack of $M > 6.5$ earthquake records. Consequently, its late Quaternary activity remains poorly constrained (Shen et al., 2003; Shi, 2021; Ren et al., 2022).

The LCJF represents the main fault within the LCJFZ (Shi, 2021). Steep terrain makes it difficult to preserve Quaternary sediments along the fault. So it is difficult to identify the marker strata for assessing its Quaternary activity. Furthermore, extensive landslides and collapse sediments can also obscure the fault trace. These challenges have led to the presumption that the fault was weak or inactive during the late Quaternary (Yu et al.,

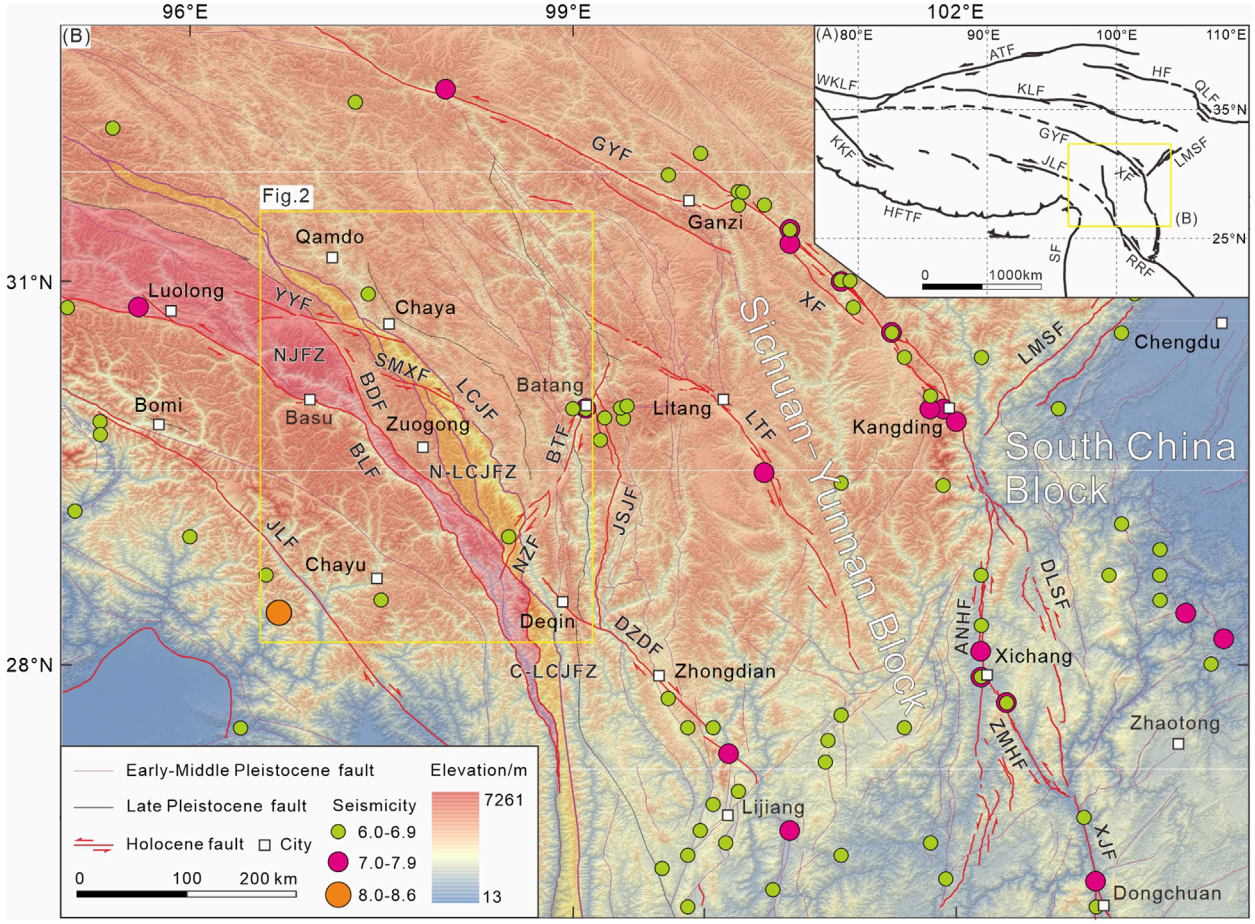

FIGURE 1
Regional tectonics **(A)** and distribution of seismicity ($M \geq 6.0$) and faults **(B)** in eastern Tibetan Plateau. Abbreviations of the major faults: WKLF, Western Kunlun fault; ATF, Altyn Tagh fault; HF, Haiyuan fault; QLF, Qinling fault; KLF, Kunlun fault; KKF, Karakorum fault; GYF, Ganzi-Yushu fault; XF, Xianshuihe fault; ANHF, Anninghe fault; ZMHF, Zemuhe fault; DLSF, Daliangshan fault; XJF, Xiaojiang fault; LMSF, Longmenshan fault; RRF, Red River fault; SF, Sagaing fault; HFTF, Himalayan front thrust fault; JLF, Jiali fault; NJFZ, Nujiang fault zone; BLF, Bianba-Luolong fault; BDF, Bangda fault; YYF, Yangda-Yaxu fault; LCJFZ, Lancangjiang fault zone; N-LCJFZ, northern segment of LCJFZ; C-LCJFZ, central segment of LCJFZ; LCJF, Lancangjiang fault; JSJF, Jinshajiang fault; DZDF, Deqin-Zhongdian-Daju fault; BTF, Batang fault; NZF, Naozhong fault; LTF, Litang fault.

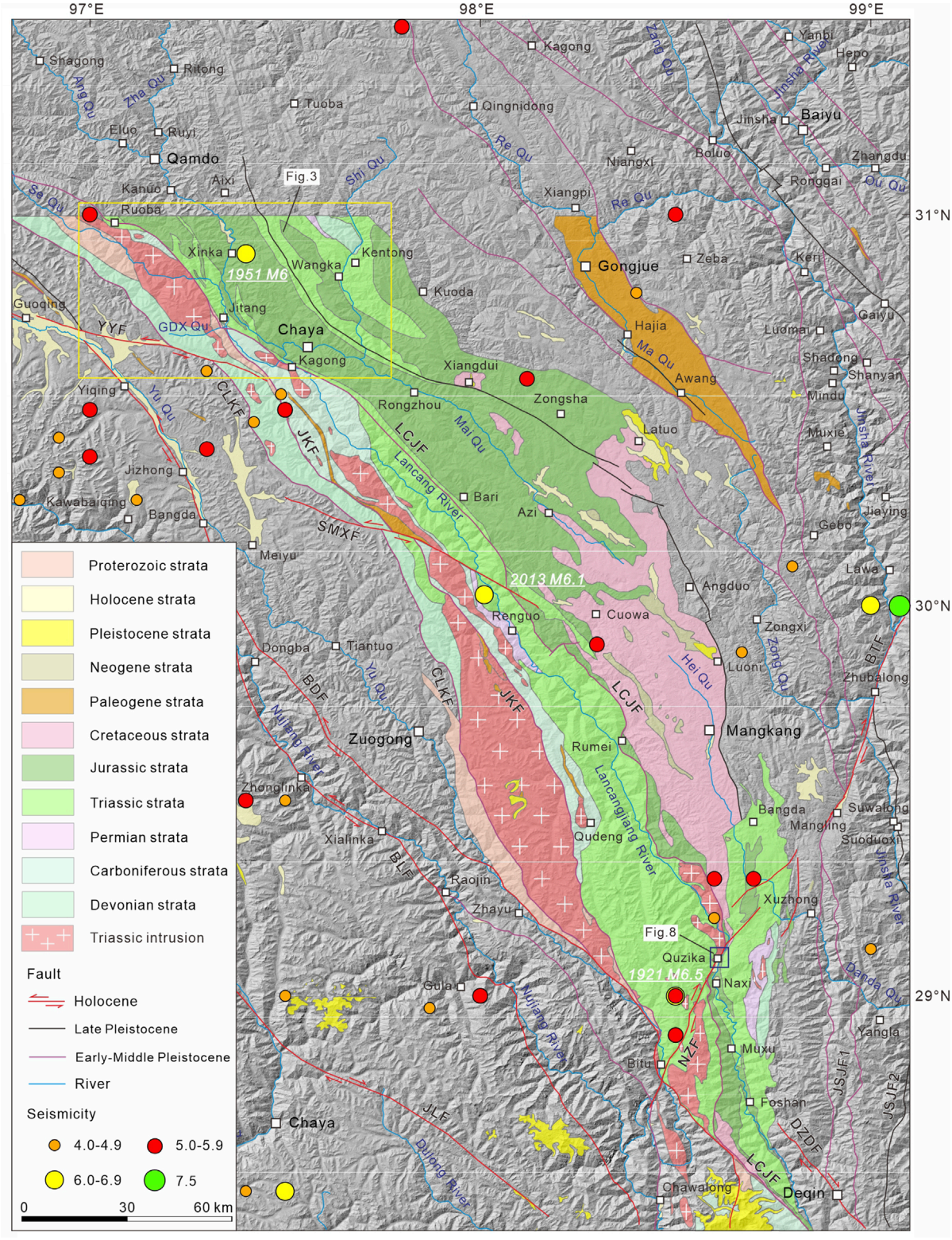

FIGURE 2
Geological features and fault distribution of Quzika-Jitang segment along the LCJFZ and adjacent region. Geological data are modified from the public 1:250,000 geological map. See the site in Figure 1. Abbreviations: JLF, Jiali fault; BLF, Bianba-Luolong fault; BDF, Bangda fault; YYF, Yangda-Yaxu fault; SMXF, Semuxiong fault; CLKF, Chalangka fault; JKF, Jiaka fault; LCJF, Lancangjiang fault; DZDF, Deqin-Zhongdian-Daju fault; JSJF1, Western boundary of Jinshajiang fault zone; JSJF2, Western branch of Jinshajiang fault zone; BTF, Batang fault; NZF, Naozhong fault; GDX Qu, Gongduoxiong Qu.

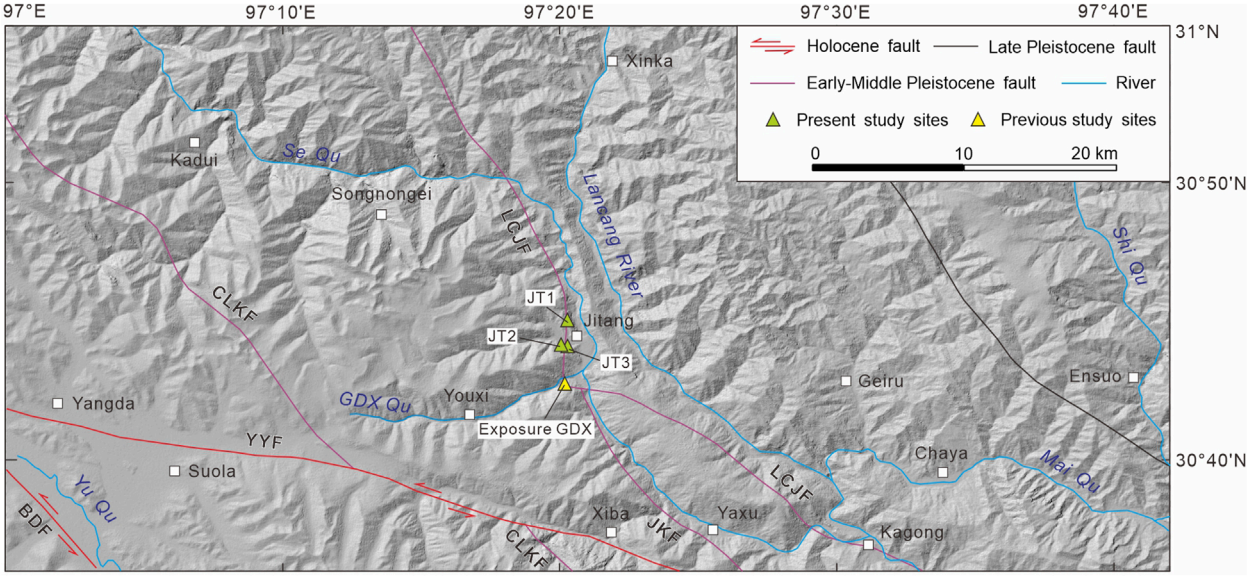

FIGURE 3
Geometry of the LCJF and distribution of study sites near Jitang Town. See the site in Figure 2. Abbreviations: BDF, Bangda fault; YYF, Yangda-Yaxu fault; CLKF, Chalangka fault; JKF, Jiaka fault; LCJF, Lancangjiang fault. GDX, Gongduoxiong.

2002; Mao et al., 2004; Wang et al., 2007). Previous studies that support this conclusion have focused primarily on the central and southern segments of the LCJF, leaving the northern segment largely uninvestigated.

Recent field surveys and trenching studies along the northern segment have documented Holocene fault activity. This interpretation, proposed by Ren et al. (2022), aligns with our trenching results at the Quzika site, which also suggest possible Holocene movement. Their conclusion is primarily supported by one outcrop (exposure GDX) located south of Jitang Town and one trench exposure (Quzika trench) located north of Quzika Township. However, the evidence from only these two sites is insufficient to assess the seismic risk of the LCJF and its role in accommodating regional crustal deformation.

In this study, we identified fault traces along the Quzika-Jitang segment through high-resolution satellite imagery and field investigations. By integrating radiocarbon dating and further verification of previously reported field observation points, we characterized the late Quaternary activity of the LCJF. Based on these findings, we further explored the patterns of strain accommodation and tectonic deformation in the Three Parallel Rivers Region during the late Quaternary.

2 Geologic setting

The Three Parallel Rivers Region, situated within the eastern segment of the Tethys-Himalayan tectonic domain, has undergone multiple phases of tectonic evolution associated with the Paleo-, Meso-, and Neo-Tethys oceanic systems (Metcalfe, 2006; Burchfiel and Chen, 2012; Pan et al., 2012; Li S. et al., 2019). Since the Cenozoic, this region has experienced intense and complex crustal deformation driven by the ongoing collision and convergence of the Indian and Eurasian plates (Tapponnier et al., 2001; Li Y. J. et al., 2019; Wang and Shen, 2020; Shen et al., 2021; Li et al., 2024). Continuous evolution and deformation have resulted in distinct topographic features, including a gradual decrease in elevation from northwest to southeast, as well as the preservation of high-elevation, low-relief landscapes characterized by alternating high mountains and deep valleys (Liu-Zeng et al., 2018; Shen et al., 2021; Cao et al., 2022). Furthermore, the tectonic evolution has nurtured a series of NW- to nearly SN-trending major strike-slip faults with arcuate geometries, such as the JSJFZ, LCJFZ, and NJFZ. These fault systems have played a fundamental role in shaping the topography, geomorphological patterns, and tectonic framework of the Hengduan Mountains Region (Yin and Harrison, 2000; Replumaz and Tapponnier, 2003; Taylor et al., 2003; Pan et al., 2012; Zhang et al., 2012; Ding and Zhong, 2013; Li et al., 2020). The interplay between these structural elements and evolving stress regimes has created the unique geological and geomorphological characteristics observed in the region today.

The LCJFZ lies within the central Three Parallel Rivers Region and generally extends in a sinuous pattern. According to its strike variation, the fault zone can be divided into three segments: the northern (NW-trending), central (NWN- to nearly SN-trending), and southern (nearly SN-trending) segments. Their boundaries are approximately delineated by Meili Snow Mountain to the north and the area between Weixi and Fengqing to the south (Figure 1; Zhong et al., 2004). This study focuses on the northern segment, specifically the region between Jitang and Quzika. Three major fault branches are identified here: the western Chalangka fault (CLKF), the central Jiaka fault (JKF), and the eastern LCJF (Figure 2; Shi, 2021).

According to existing 1:250,000 geological map data (Figure 2), bedrock units in the northern segment and adjacent areas primarily comprise Proterozoic Jitang Group (gneiss) and Youxi Group

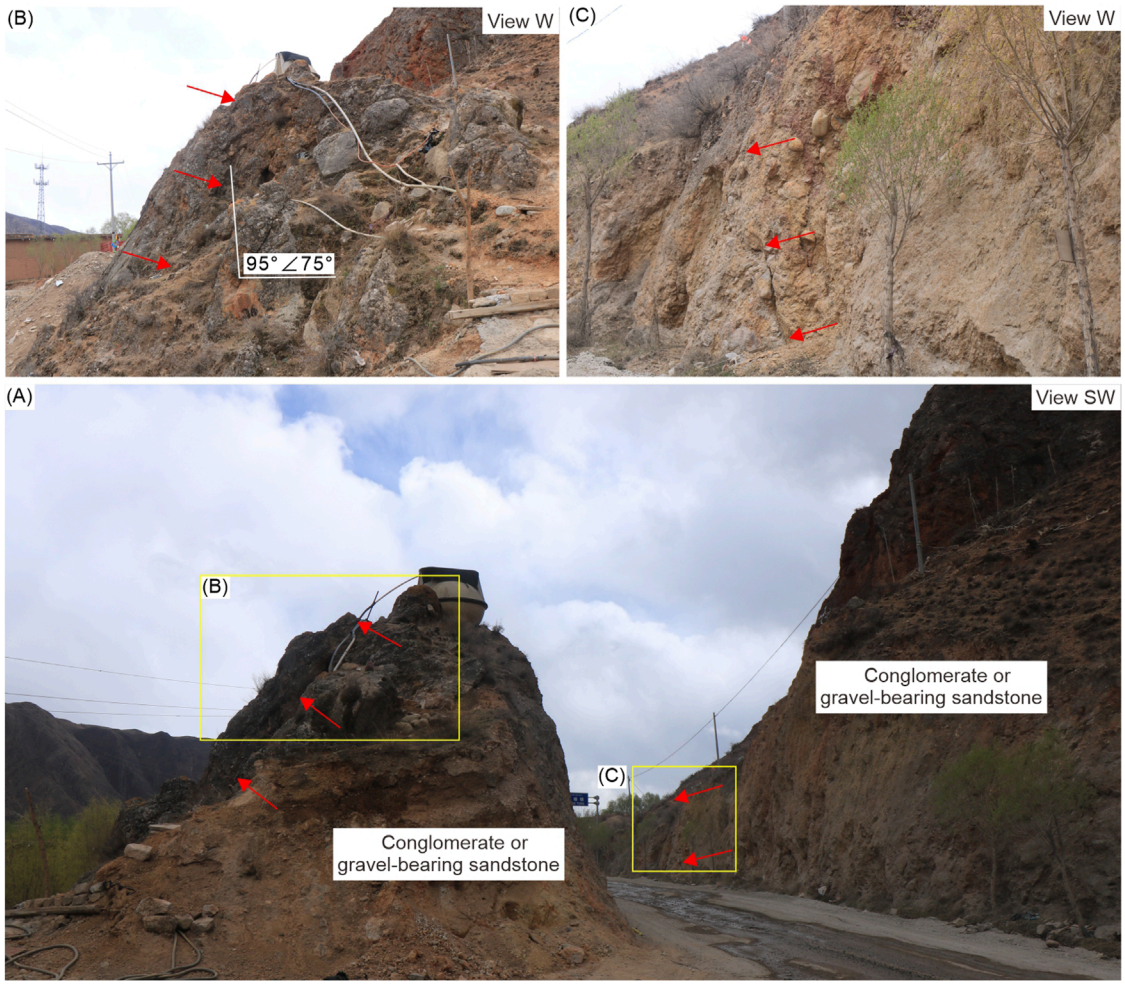

FIGURE 4
Macro **(A)** and close-up **(B,C)** photographs of exposure JT1 near Jitang Town. See the site in Figure 3. Red arrows present the fault trace.

(schist). Mesozoic strata constitute the dominant lithological units within the study area and delineate the principal trace of the eastern branch fault. These strata exhibit a striking contrast on either side of the fault, with Jurassic formations (Dongdaqiao, Wangbu, and Xiaosuoka Formations) predominantly exposed on the eastern side, while the Middle-Late Triassic Zhuka Group mainly characterizes the western side. Late Paleozoic strata exhibit the second most extensive distribution after the Mesozoic units, occurring predominantly west of the LCJF. Early Paleozoic strata are absent in the study area. Late Quaternary deposits primarily consist of terrace and gully alluvial sediments. Their distribution is restricted, with the main occurrences clustered near Jitang Town and Quzika Township. Late Triassic adamellite and granodiorite intrusions occur predominantly west of the LCJF.

The Cenozoic movement of the LCJFZ was predominantly characterized by strike-slip and thrust properties, which controlled the development of several small Paleogene basins and the folding deformation of Paleogene strata on both sides (Wang et al., 2001; Zhong et al., 2004). From the Eocene to the Miocene, the fault zone mainly exhibited sinistral strike-slip characteristics (Wang et al., 2008; Zhang et al., 2009). Since the Quaternary, evidence has indicated a shift to dextral strike-slip motion (Duan and Tan, 2000). In the late Quaternary, research has primarily focused on its three branch faults, with the most extensive studies conducted on the eastern branch. Geomorphic features, geological profiles, and chronological data suggest that the western and central branches were inactive during this period (Shi, 2021). In the early stage, most work presumed that the main active period of this fault was Early to Middle Pleistocene, with some segments possibly active in the early Late Pleistocene (Yu et al., 2002; Mao et al., 2004; Wang et al., 2007). Some studies also suggested that there were geomorphic signs of Late Pleistocene-Holocene activity near Yanjing Town (now known as Naxi Township), indicating that the fault was a Holocene active fault with both normal and right-lateral strike-slip characteristics, and might act as the western boundary of the Sichuan-Yunnan rhombic block (Shen et al., 2003). With ongoing research, progress has been achieved in recent years. Our trench exposures near Quzika Township revealed multiple displacements of Holocene strata. Subsequent research by Ren et al. (2022) reported that the LCJF (also called Baqing-Leiwuqi fault) offset Holocene terraces and slope alluvial fans north of Chaya. Additionally, an outcrop at the fan edge showed that gravel clasts in layer U2 exhibit a preferred orientation. These findings collectively constrain the fault's Holocene seismogenic potential.

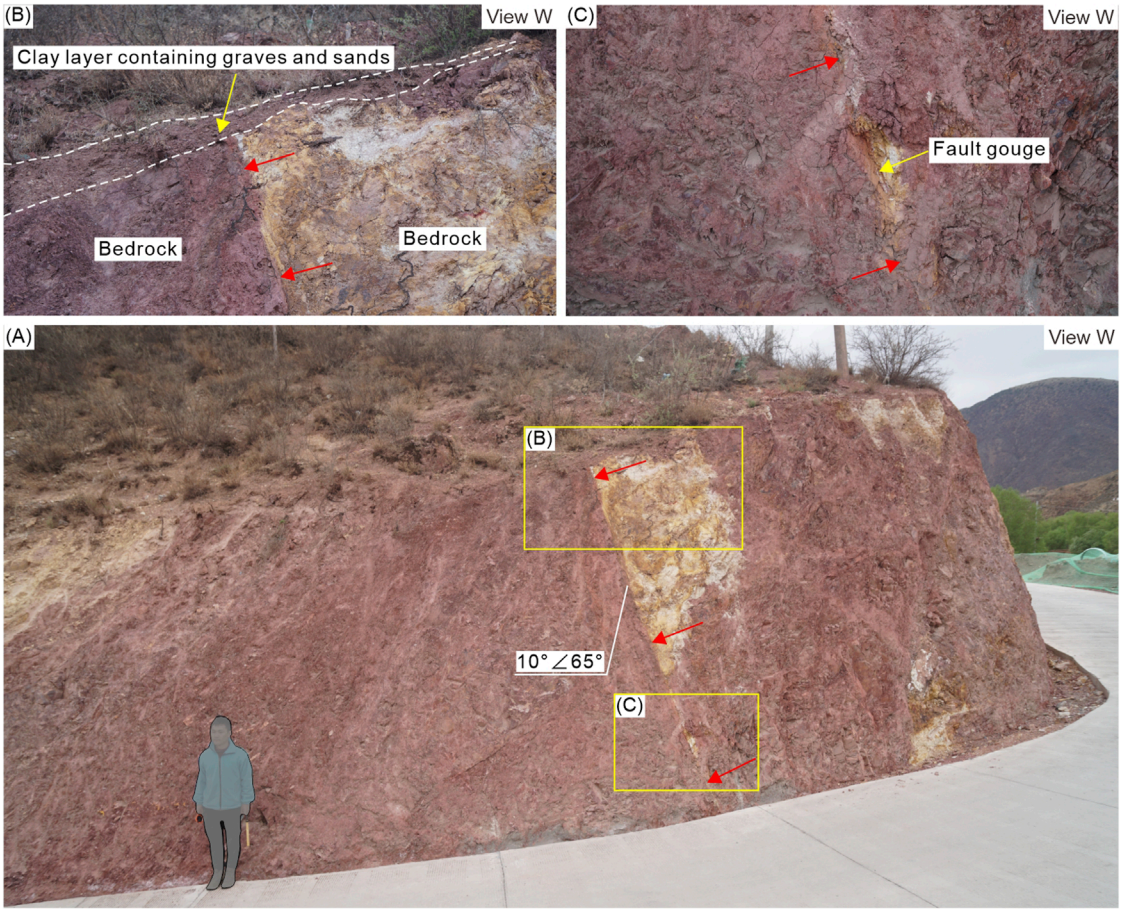

FIGURE 5
Macro **(A)** and close-up **(B,C)** photographs of exposure JT2 near Jitang Town. See the site in Figure 3. Red arrows present the fault trace.

However, based on low-temperature thermochronology data and thermodynamic models, Li et al. (2024) acknowledged that the LCJF (Baqing-Leiwuqi fault) has not been very active since ~10 Ma, and may have even ceased activity.

The LCJFZ has experienced relatively low seismic activity. Historical records indicate no $M > 6.5$ earthquakes along the LCJFZ. The three largest earthquakes are the 1921 M 6.5 earthquake, the 1951 M 6 earthquake near Qamdo, and the 2013 M 6.1 earthquake in Zuogong (Figure 2). In addition, a few moderate earthquakes with a magnitude of 5.0–5.5 have occurred occasionally (Science and Technology Committee of the Tibetan Autonomous Region, 1982; Department of Earthquake Disaster Prevention State Seismological Bureau, 1995). These moderate to strong earthquakes are mainly distributed along the LCJF, particularly concentration near the Quzika site (Figure 2).

3 Typical fault outcrops and tectonic landforms

The LCJF primarily develops within Pre-Cenozoic bedrock and exhibits significant topographic and geomorphological contrasts as well as pronounced erosion in the study area. Late Quaternary strata are poorly preserved along the fault trace. According to publicly available 1:250,000 geological map data, the sites of Jitang, Gongduoxiong, and Quzika were selected as the primary study locations for their extensive distributions of late Quaternary sediments (Figure 2).

3.1 Jitang site

Near Jitang Town, three fault exposures were distributed along the mountain front on the right bank of Se Qu (Figure 3). One exposure, denoted as JT1, is located north of the town (Figures 3, 4). The other two exposures, situated to the south, are spaced within a straight-line distance of no more than 100 m apart and are labeled JT2 and JT3 from west to east (Figures 3, 5, 6).

Exposure JT1, in the Pliocene to early Quaternary purple-red semi-consolidated conglomerate or gravel-bearing sandstone, reveals multiple small-scale, nearly north-south trending fault planes (Figure 4). Well-developed terraces (T1 and T2 of Se Qu) are present just north of exposure JT1. No evidence of faulting or deformation was observed on the terrace surfaces, suggesting that the most recent activity of the LCJF at this location should have occurred prior to the formation of the terrace T2.

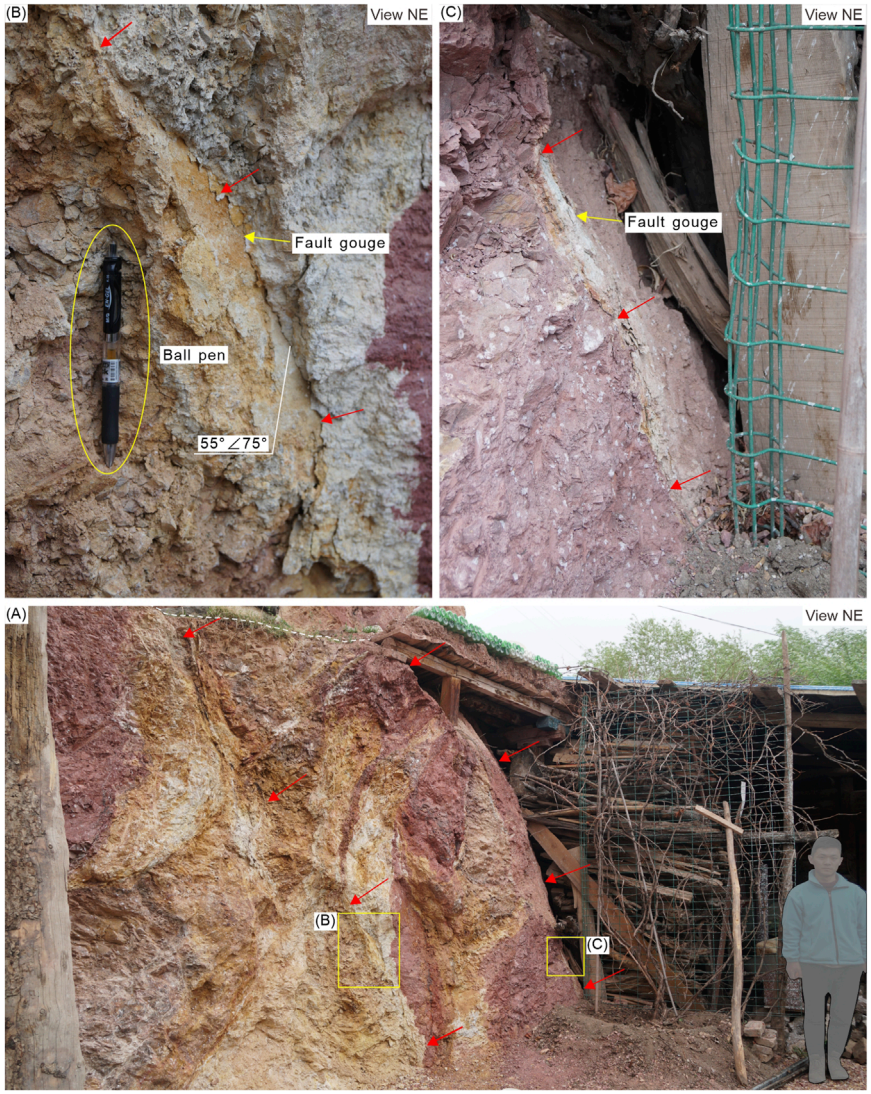

FIGURE 6
Macro **(A)** and close-up **(B,C)** photographs of exposure JT3 near Jitang Town. See the site in Figure 3. Red arrows present the faults. White dashed line presents the ground surface.

Exposure JT2, developed within the purple-red sandstone, exposes a well-defined fault plane (Figure 5). A thin layer of yellow to earthy-yellow, semi-consolidated fault gouge borders the fault plane. The fault offsets the purple-red sandstone and is overlain by thin layers of clay to sub-clay containing gravel and sand (Figure 5). Exposure JT2 is situated on the edge of a large, approximately east-west-trending gully on the right bank of Se Qu. The thin layers of clay to sub-clay in the upper part of the exposure represent the late Quaternary alluvial deposits from the gully. Based on the cut-and-fill relationship observed, we infer that the LCJF has been inactive at this location since the late Quaternary.

Exposure JT3 also consists of fractured bedrock (Figure 6). Two steeply dipping, nearly parallel faults were identified, which cut through purple-red to earthy-yellow bedrock strata and extend upward to the ground surface. The faults have well-defined planes with an attitude of 55°∠75°. Along the fault planes, semi-consolidated fault gouges are present, exhibiting a grayish-green to earthy-yellow color and a thickness on the millimeter scale. The absence of Quaternary strata at the top of the exposure precludes a direct assessment of late Quaternary fault activity. However, the highly consolidated nature of the fault gouges suggests that the most recent activity of the LCJF at this site likely predates the late Quaternary.

3.2 Gongduoxiong site

The Gongduoxiong (GDX) Qu, located southwest of Jitang Town, is a tributary of the Se Qu (Figure 3). Previous studies by Ren et al. (2022) proposed that the LCJF traverses the approximately EW-trending GDX Qu, displacing both the floodplain T0 and terrace T1 on its left bank, as well as a slope-derived alluvial fan

10.3389/feart.2025.1667992

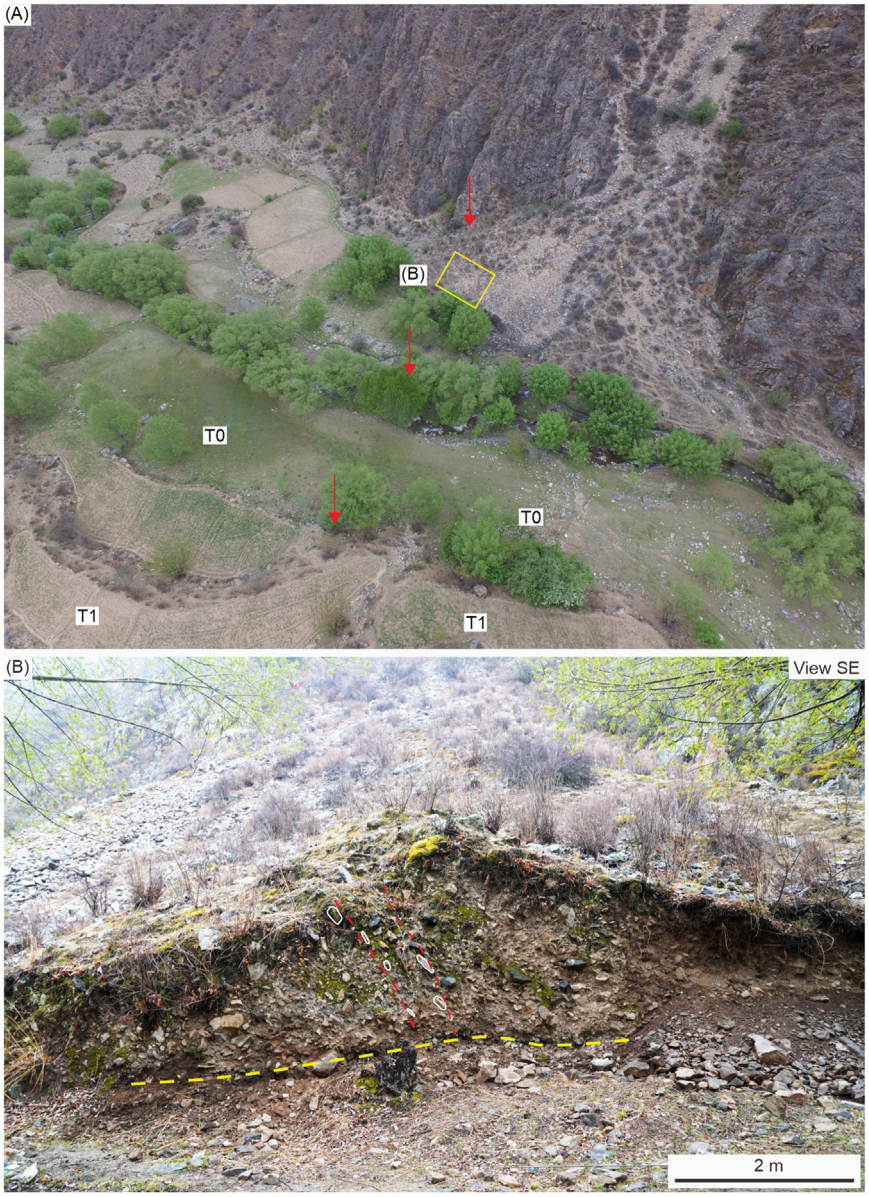

FIGURE 7
Landform **(A)** and exposure **(B)** near the GDX Qu. See the site in Figure 3. Red arrows **(A)** and dashed lines **(B)** indicate the fault trace identified by Ren et al. (2022). White ellipses represent aligned gravels. Yellow dashed line represents the lower bound of aligned gravels.

on its right bank (Figures 3, 7A). The exposure GDX, situated at the margin of this alluvial fan, shows multiple aligned gravels (Figures 3, 7B). Combining these field observations with a landform located north of Jitang Town, Ren et al. (2022) concluded that the LCJF was a Holocene active fault.

Through integrated analysis of satellite imagery and field investigations at exposure GDX and adjacent geomorphic features, along with bedrock exposures on both sides, as documented by Ren et al. (2022), we obtained the following findings: (1) No fault plane was identified within exposure GDX. The aligned gravels are locally developed and restricted to the upper and middle parts, and are absent in the lower part (Figure 7B). (2) Exposure GDX is located on the mountain-front alluvial fan (Figure 7A), and the locally observed aligned gravels resulted from multiple episodes of fan deposition rather than tectonic activity, as the so-called "fault planes" do not extend downward (Figure 7B). (3) Within bedrock exposures on both sides, no significant fault fracture zones were identified. Only minor joints and cleavages, with a width of approximately 20–30 cm, were observed in the stratigraphic sections. These characteristics obviously mismatch with the scale of the LCJF. (4) The floodplain T0, terrace T1, and the alluvial fan equivalent to terrace T2 on the left bank of GDX Qu maintain structural continuity without discernible fault displacement. Thus, based on these direct observations, we conclude that it is not sufficient to consider the exposure GDX as geological evidence for Holocene activity of the LCJF.

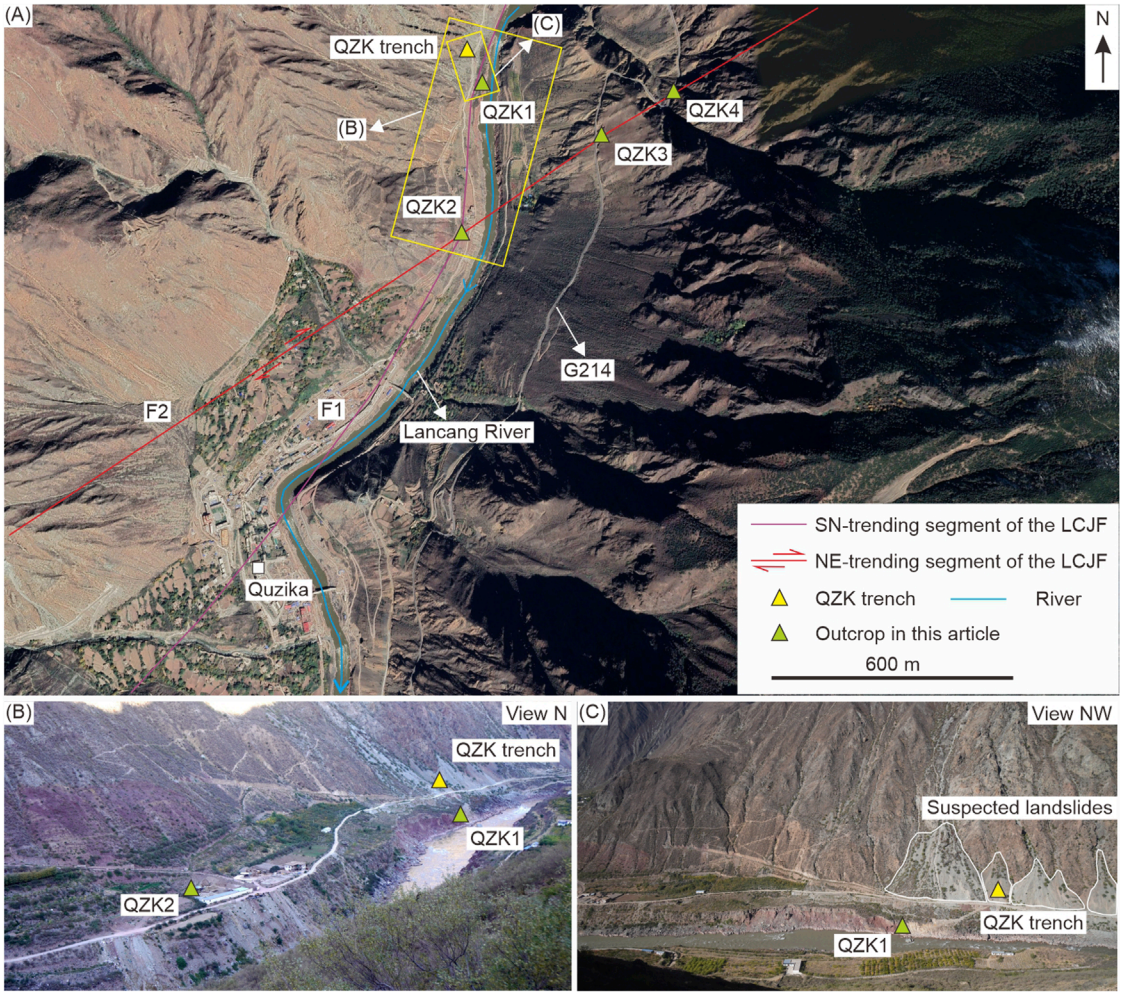

FIGURE 8
Study sites and local geomorphology near Quzika Township. **(A)** Survey points of current and previous study. **(B)** Exposures QZK1 and QZK2 and adjacent geomorphology. **(C)** Local geomorphology around QZK Trench.

3.3 Quzika site

Near Quzika Township, four fault exposures were discovered on both sides of the Lancang River, with two on the left bank, denoted as QZK1 and QZK2 from north to south, and the other two on the right bank as QZK3 and QZK4 from west to east (Figure 8).

Exposure QZK1, located about 2.6 km north of Quzika Township, is characterized by intense compression and fracturing over a length of approximately 20 m (Figure 9). The exposure consists primarily of bedrock strata overlain by gravel layers, with the exception of a set of sand layers in the upper part. According to consolidation degree, the gravel layers can be divided into two distinct units, with a semi-consolidated gravel layer in the lower part and a loose gravel layer in the upper part, which form an unconformity (Figures 9A,B). The exposure clearly reveals multiple nearly SN-trending faults, roughly including two groups, one dipping south and the other dipping north, both of which have steep dips (Figure 9A). Yellow-white, semi-consolidated fault gouges are present along the fault planes (Figures 9A,C). The southward dipping faults are relatively old and are overlain by the semi-consolidated gravel layer, while the northward dipping faults are younger and cut through both the bedrock strata and overlying semi-consolidated gravel layer, and are subsequently overlain by loose gravel layers (Figure 9B). Specifically, at the southwest end of the exposure, the most recent fault activity has disturbed the semi-consolidated gravel layer, resulting in significant rotational deformation and a preferred orientation of multiple pebbles along the fault plane (Figures 9A,B).

Exposure QZK2, located approximately 700 m south of QZK1, has been widely exposed by human activity at the southeast corner of the terrace T1 surface. The exposure is approximately 16–17 m long, and 5–6 m deep (Figure 10). The strata in the exposure consist mainly of gravel layers containing sand and sandy soil, exhibiting a roughly interbedded sedimentary structure (Figures 10A,B). On the basis of stratigraphic features, five sets of layers (including eight subunits) were recognized and are named from bottom to top (Figure 10B). Three NE-trending reverse faults with gentle dips were recognized based on characteristics such as stratigraphic faulting, traction deformation, and aligned gravels. Each fault contains two

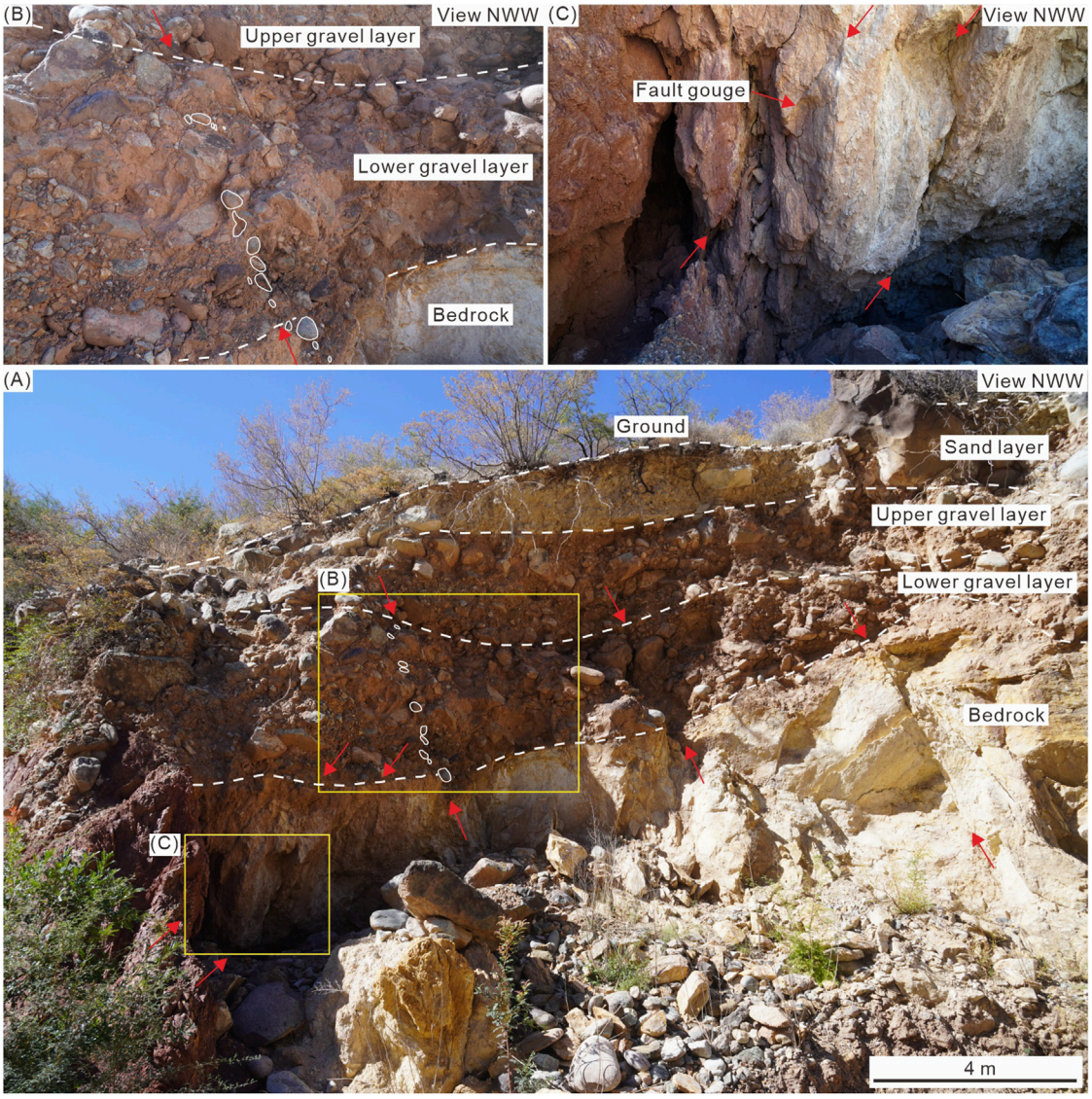

FIGURE 9
Macro **(A)** and close-up **(B,C)** photographs of exposure QZK1 near Quzika Township. Red arrows present the fault trace. White ellipse present aligned gravels.

branches (Figure 10B). Faults F2-3 and the southeast branch of F2-2 simultaneously offset multiple strata, namely, layers U2a, U2b, U3a, U3b, U4a, and U4b, and are overlain by the clayey sandy gravel layer U5. In addition, aligned gravels are also vaguely visible along the fault planes. Notably, the marker layer U2b exhibits significant folding and displacement across fault F2-2. It is almost horizontal on the southeast side but is noticeably inclined on the northwest side, with a thrust value of approximately 1.5 m (Figure 10C). These characteristics suggest that this NE-trending fault may have been active during the Holocene.

To constrain the latest activity of this event, an organic-rich soil sample was collected from the central sector of layer U4a for radiocarbon dating (Figure 10B). This age suggests that the most recent faulting event occurred after 920 ± 30 years BP. However, according to field investigation data, the interference of landslides cannot be ruled out (Figure 8C).

Farther northeast, ~800 m, exposure QZK3 is a bedrock section revealing a clear fault zone. This zone extends toward the ground surface with a NE trend and a steep dip (Figures 11A,B). A thin layer of transparent gypsum fills the fault zone, with a thickness of about 2–4 cm (Figure 11C).

Located approximately 300 m farther to the northeast, exposure QZK4 reveals multiple NE-trending faults with clear fault planes (Figure 12). Along some of the fault planes, a small amount of highly consolidated fault gouge is present (Figure 12A). After having cut through the bedrock, the faults exhibit different characteristics. The northern branch is overlain by terrace deposits, while the southern branch continues upward, cutting through

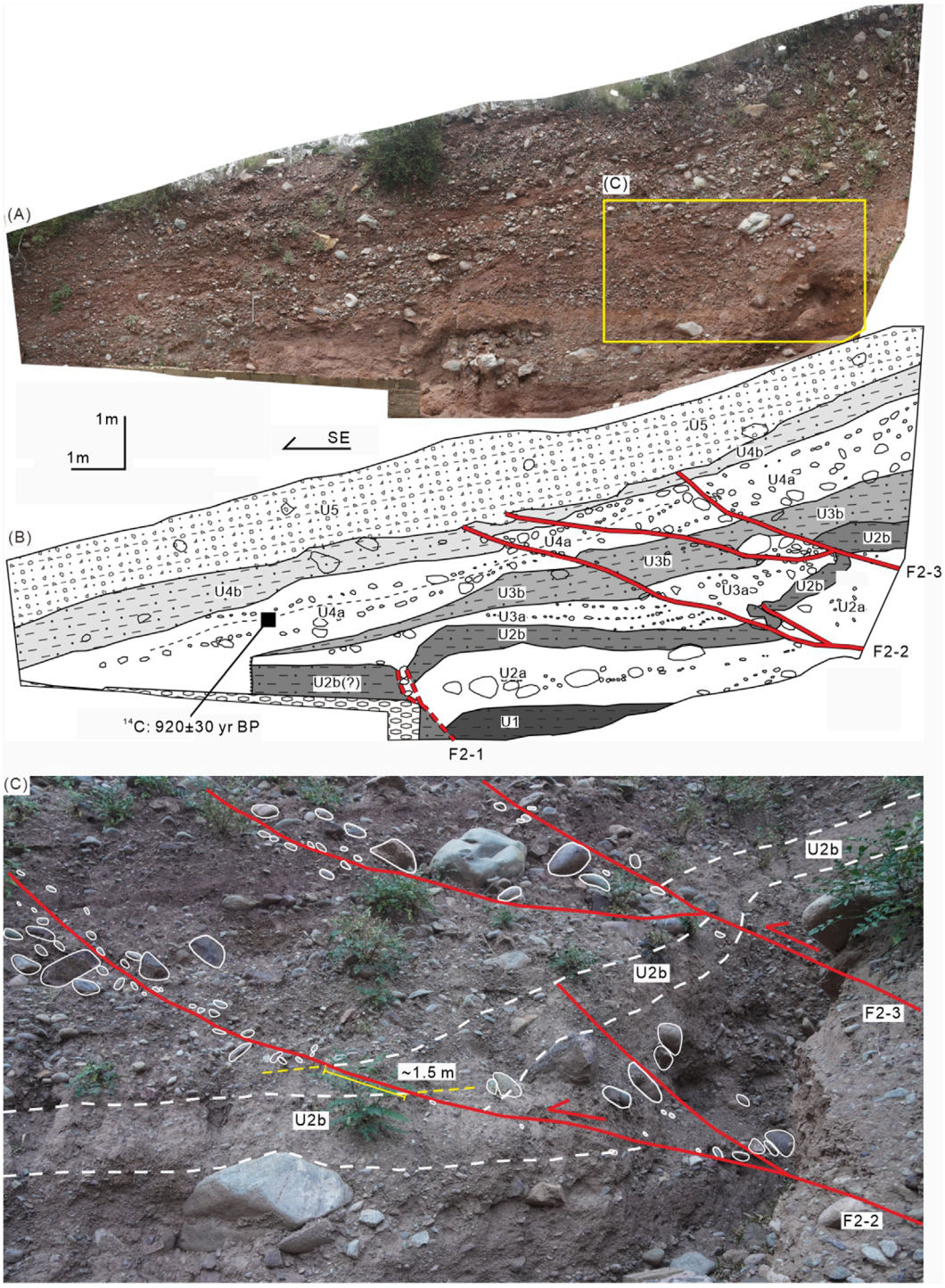

FIGURE 10
Photograph **(A)** and interpreted sketch **(B)** of the exposure QZK2. **(C)** Enlarged photograph showing local details. U1, sandy clay interbedded with sparse fine gravel; U2a, sandy gravel layer with poorly sorted, subrounded clasts, exhibiting sub-horizontal bedding. Near the fault zone, the deposits display chaotic, structureless fabric; U2b, brick-red sandy clay with sparse fine gravel and abundant carbonaceous fragments; U3a, wedge-shaped gravel layer, containing subordinate amounts of large gravel (up to ~10 cm diameter). Near the fault, deposits exhibit increased gravel content, poor sorting, and chaotic fabric, whereas distal areas display slope-parallel bedding; U3b, sandy clay interbedded with gravel layers, exhibiting slope-parallel bedding; U4a, sandy gravel layer with locally interbedded thin sandy-clay, exhibiting slope-parallel bedding; U4b, sandy clay interbedded with subordinate gravel, exhibiting slope-parallel bedding; U5, clayey gravel layer with subrounded clasts.

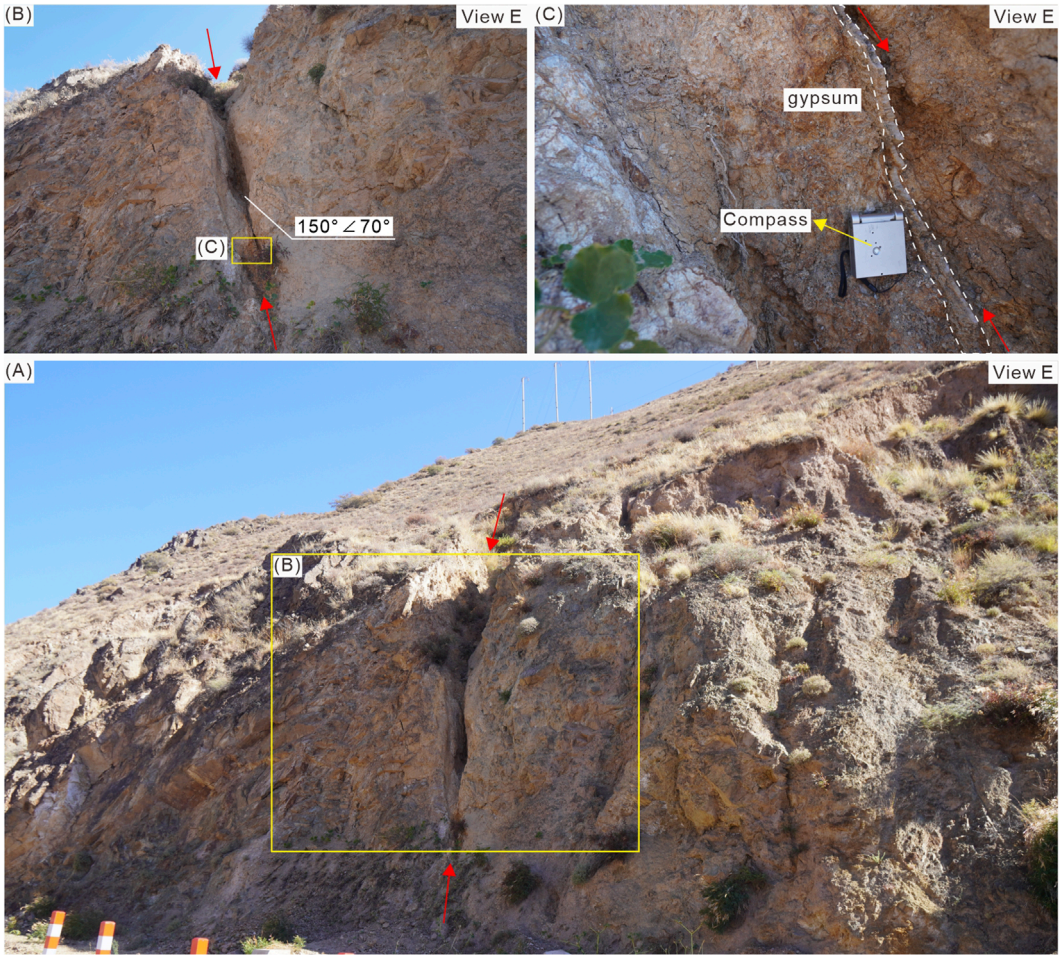

FIGURE 11
Macro photograph **(A)** and successive close-up photographs **(B,C)** of exposure QZK3 near Quzika Township. Red arrows present the fault trace.

residual and slope deposits and resulting in a preferred orientation of gravels (Figures 12B,C).

4 Discussion

4.1 Late quaternary activity characteristics of the LCJF

Through detailed field investigations, we identified seven fault exposures at the Jitang and Quzika sites. Exposures JT1 through JT3 and QZK1 reveal that the Quzika-Jitang segment of the LCJF generally trends SN (denoted as F1; Figures 8, 13), manifested as a complex structural system composed of several branches, with widths ranging from several to approximately 20 m (Figures 4–6, 9). The remaining three exposures, QZK2 through QZK4, show that the LCJF also features a NE-trending branch fault (recorded as F2) near the Quzika site (Figures 8, 10–13).

4.1.1 Nearly SN-trending segment (fault F1)

Fault F1 cuts through both bedrock and semi-consolidated Pliocene to Early Quaternary conglomerate or gravel-bearing sandstone, and is unconformably overlain by a sequence of loose gravel layers or by late Quaternary thin layers of clay to sub-clay with gravel (Figures 4–6, 9). Exposure JT1 further reveals that the most recent activity of fault F1 did not affect terrace T2 of Se Qu, located north of the exposure (Figure 4). Additionally, exposures JT2, JT3 and QZK1 show that semi-consolidated fault gouge is present along multiple fault planes (Figures 5, 6, 9). Although quantitative age constraints are currently lacking, the degree of consolidation of the fault gouge suggests that the most recent fault activity likely predated the late Quaternary.

The above findings contradict previous viewpoints. Field investigations at the southern Jitang site (Ren et al., 2022) and the Quzika site (our team) suggest that fault F1 offsets Holocene strata, indicating Holocene activity. The primary supporting evidence consists of exposure GDX (Figure 7; Ren et al., 2022) and the Quzika trench, which represent the only two pieces of geological evidence cited for Holocene activity on F1. This study conducted field investigations on exposure GDX, as identified by Ren et al. (2022). We argue that the field observations at the GDX site cannot be regarded as definitive geological evidence for Holocene activity of the LCJF (Figure 7). Due to inaccessible roads, field

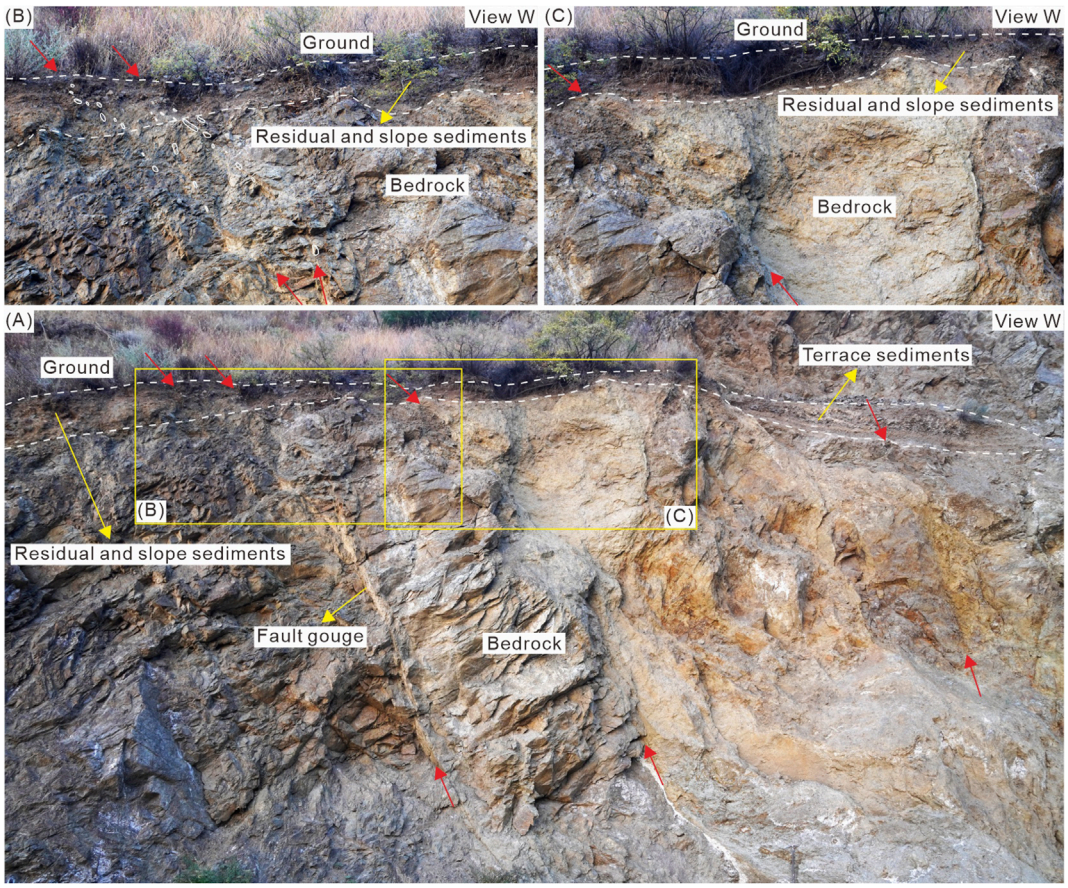

FIGURE 12
Macro **(A)** and close-up **(B,C)** photographs of exposure QZK4 near Quzika Township. Red arrows present fault trace. White ellipses represent aligned gravels.

surveys could not be performed at the Quzika trench and its surrounding landforms (Figure 8). However, based on satellite image interpretation (Figure 8C) and existing knowledge from peer studies, the possibility of landslide interference cannot be ruled out. In summary, there is currently no conclusive evidence supporting Holocene activity along fault F1. Combined with previous research, our findings lead us to infer that the nearly SN-trending fault F1 has been inactive since the late Quaternary. This interpretation is further supported by (1) the limited seismic activity along the LCJF (Figures 1, 2) and (2) recent thermochronological data and thermodynamic modeling results published by Li et al. (2024).

On the other hand, fault F1 features a relatively wide fault zone, spanning several to approximately 20 m in width. It is characterized by semi-consolidated fault gouge along its fault planes and intense bedrock fragmentation within and adjacent to the zone (Figures 4–6, 9–12). Additionally, fault F1 exerts a strong control on the differential distribution of stratigraphic units on both sides (Figure 2). Together, these observations suggest that although fault F1 has been inactive since the late Quaternary, it represents a major structure that was active during earlier geological periods, from at least the Pliocene to the Early Quaternary.

4.1.2 NE-trending segment (fault F2)

At the Quzika site, three fault exposures (QZK2, QZK3 and QZK4) are well-exposed within a linear distance of approximately 1.1 km (Figure 8). These exposures exhibit a consistent NE-trending linear distribution. The fault planes all strike NE (Figures 10–12). These results confirm the presence of a NE-trending fault (F2) near Quzika Township. In fact, although fault F2 has been previously recognized, the lack of exposure data has hindered verification of its activity. This study provides geological exposure evidence for the first time.

The three fault exposures reveal that fault F2 may have been active during the late Quaternary (Figures 10–12). Specifically, exposure QZK2 shows that faults F2-2 and F2-3 have displaced multiple sandy gravel layers and clay to sub-clay units, including layer U4a (Figure 10). Layer U2b exhibits the most pronounced offset, with a thrust displacement of approximately 1.5 m along fault F2-2 (Figure 10C). A radiocarbon age obtained from layer U4a constrains the timing of faulting, indicating that the most recent fault movement occurred after approximately 920 years BP (Figure 10B). Furthermore, exposure QZK4 shows that the southern branch fault has displaced loose Quaternary deposits overlying the bedrock (Figures 12A,B).

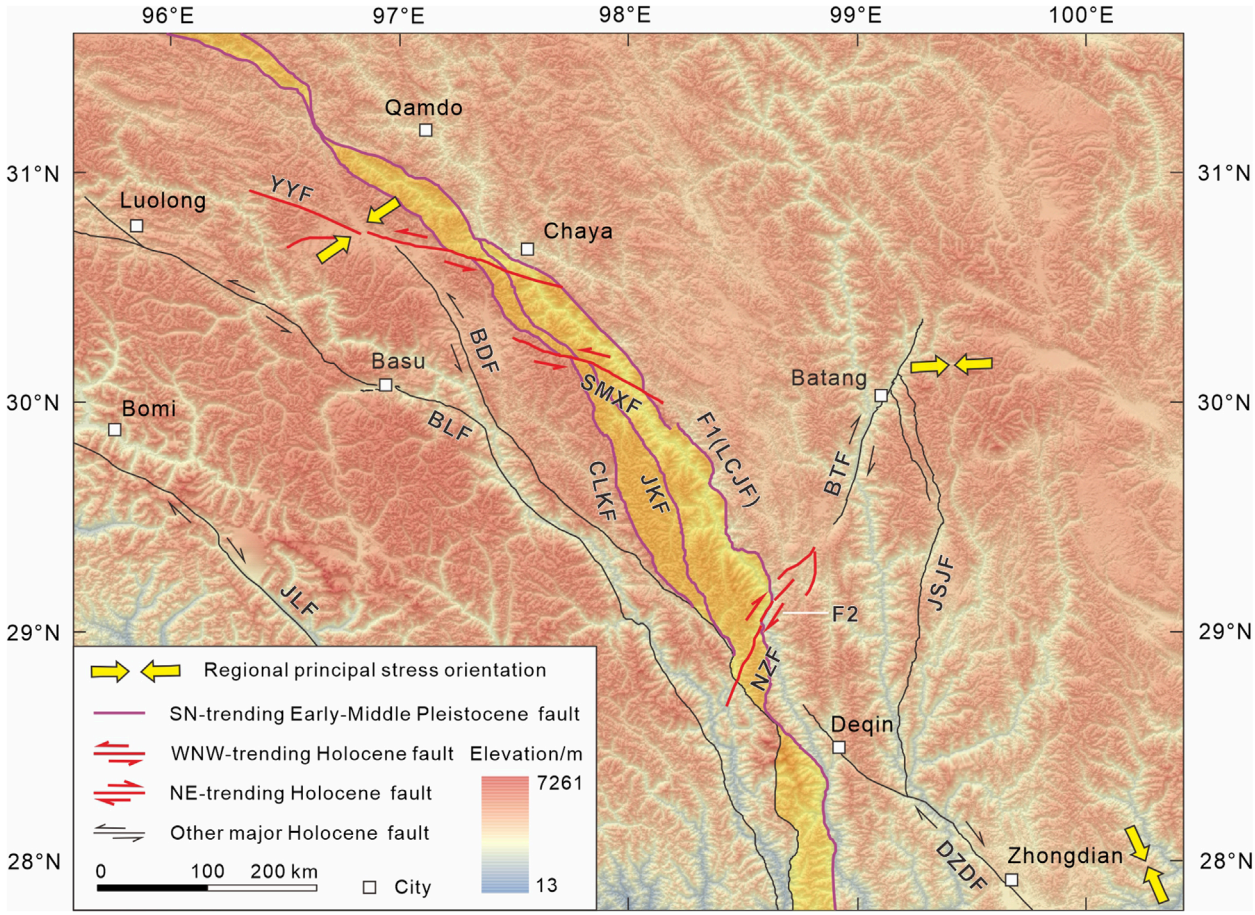

FIGURE 13
A schematic model of regional tectonic deformation. The yellow-shaded area represents the LCJFZ. Stress field data are from Kan et al. (1983), Xu et al. (1987), and Heidbach et al. (2018). Abbreviations of faults: JLF, Jiali fault; BLF, Bianba-Luolong fault; BDF, Bangda fault; YYF, Yangda-Yaxu fault; SMXF, Semuxiong fault; CLKF, Chalangka fault; JKF, Jiaka fault; LCJF, Lancangjiang fault; F1, SN-trending segment of the LCJF; F2, NE-trending segment of the LCJF; NZF, Naozhong fault; DZDF, Deqin-Zhongdian-Daju fault; JSJF, Jinshajiang fault; BTF, Batang fault.

Additionally, historical records document an *M* 6 earthquake near Yanjing (now known as Naxi), about 6 km south of Quzika Township, which occurred in 1920 (Liu, 1991). Further geomorphic evidence indicates the presence of an NE-trending active fault near this location (Shen et al., 2003). These seismic and geomorphic observations collectively suggest potential Holocene activity along fault F2.

Currently, no consensus exists on the tectonic affiliation of fault F2. While some researchers attribute it to the LCJF system (Shen et al., 2003), others interpret it as the southern extension of the Batang fault (Chayu and Dangxiong earthquake investigation teams in Xizang, 1987; Zhang et al., 2024), alternatively referred to as the Naozhong fault (Figures 1, 2, 13; Zhang P. Z. et al., 2022). Most importantly, integrated seismic, geomorphological, and geological evidence provide strong constraints on the existence of a NE-trending fault that was active in the late Quaternary near the Quzika site, irrespective of its tectonic classification.

4.2 Implications for regional tectonic deformation patterns

Our new findings and previous work (Shi, 2021) indicate that the three main branches of the LCJFZ have shown no discernible activity during the late Quaternary. Consequently, the LCJFZ has likely remained tectonically inactive since this period and no longer acts as the primary structure accommodating regional crustal deformation. The study area occupies a critical position within the tectonic framework of the eastern Tibetan Plateau, which is characterized by eastward extrusion and clockwise rotation (Armijo et al., 1989; Tapponnier et al., 2001; Burchfiel and Chen, 2012; Wang and Shen, 2020; Shen et al., 2021; Zhang D. et al., 2022). This region plays a pivotal role in absorbing and regulating strain associated with (1) transpressional deformation from the oblique convergence between the Indian and Eurasian plates, and (2) the southward migration of Plateau material. A key question thus emerges: by what mechanism has this region accommodated and partitioned intense

tectonic deformation since the late Quaternary, given the apparent quiescence of the LCJFZ?

Our observations reveal a NE-trending fault (F2) near Quzika, which we interpret as a secondary structure of the LCJFZ. This secondary fault cuts through the main fault zone and exhibits clear evidence of late Quaternary activity. Similarly, the WNW-trending Yangda-Yaxu fault (YYF) intersects the LCJFZ (Han et al., 2022b; Li et al., 2024). Although relatively small in scale, the YYF has been highly active during the late Quaternary, not only generating multiple destructive earthquakes but also causing synchronous displacement along multiple LCJFZ branches (Han et al., 2022b; Ren et al., 2022). Its intersecting relationships with the pre-existing LCJFZ, coupled with systematic low-temperature thermochronology data, strongly suggest that this branch fault is a newly developed structure (Han et al., 2022b; Li et al., 2024). We therefore propose that the WNW-trending YYF and the NE-trending F2 are currently the most active structures around the LCJFZ. Furthermore, a WNW-trending fault (designated as SMXF; Figures 1, 2, 13) is developed approximately 50 km south of the YYF. Preliminary investigations have suggested potential Holocene activity along this fault (Li, 2019). Given the inconclusive nature of the available evidence, this fault was excluded from detailed analysis in the present study. Collectively, these facts highlight that the main structures absorbing and regulating regional deformation have switched from the nearly SN-trending LCJFZ to several secondary faults, including the WNW-trending YYF and the NE-trending F2. This indicates that tectonic transformation and fault neogenesis may have occurred around the LCJFZ (Figure 13). Multiple lines of evidence—including focal mechanism solutions, seismic deformation zone kinematics, crustal deformation field analyses, and *in-situ* stress measurements—indicate a dynamic evolution of the stress regime along the eastern-southeastern Tibetan Plateau margin during successive geological epochs (Kan et al., 1983; Xu et al., 1987; Heidbach et al., 2018; Wang and Shen, 2020). We propose that temporal variations in the regional stress field may be the primary driver of this tectonic transformation (Figure 13). However, we emphasize that this interpretation remains provisional. Fundamental questions persist—most notably regarding the exact timing and dynamic mechanisms underlying this transition—and require rigorous multidisciplinary investigation.

5 Conclusion

Based on extensive fieldwork, radiocarbon dating, and synthesis of prior research, we propose the following three preliminary conclusions:

1. The approximately SN-trending main fault of the LCJF (F1) was active from the Pliocene to the Early Quaternary but shows no evidence of activity since the late Quaternary.
2. A NE-trending branch fault (F2) within the LCJFZ near Quzika Township displaces late Quaternary strata and may have Holocene activity.
3. Since the late Quaternary, the role of the LCJFZ in accommodating regional deformation has diminished. Newly formed secondary strike-slip faults that intersect the LCJFZ now exhibit significant activity and have become the primary structures accommodating regional tectonic strain. This shift indicates a tectonic reorganization from the approximately SN-trending LCJFZ to several secondary faults, suggesting that tectonic transformation and fault neogenesis have likely occurred in the vicinity of the LCJFZ.

Data availability statement

The datasets presented in this study can be found in online repositories. The names of the repository/repositories and accession number(s) can be found in the article/supplementary material.

Author contributions

MH: Data curation, Investigation, Writing – original draft, Writing – review and editing. SW: Formal Analysis, Investigation, Writing – review and editing. YL: Investigation, Writing – review and editing. LC: Conceptualization, Funding acquisition, Investigation, Writing – review and editing. XL: Data curation, Writing – review and editing. DW: Formal Analysis, Writing – review and editing. XZ: Investigation, Writing – review and editing.

Funding

The author(s) declare that financial support was received for the research and/or publication of this article. This research was supported financially by the Second Tibetan Plateau Scientific Expedition and Research Program (STEP) (2019QZKK0901); Spark Program of the China Earthquake Administration (XH24036B); and State Key Laboratory of Earthquake Dynamics, Institute of Geology, CEA (LED2024B02).

Conflict of interest

The authors declare that the research was conducted in the absence of any commercial or financial relationships that could be construed as a potential conflict of interest.

Generative AI statement

The author(s) declare that no Generative AI was used in the creation of this manuscript.

Any alternative text (alt text) provided alongside figures in this article has been generated by Frontiers with the support of artificial intelligence and reasonable efforts have been made to ensure accuracy, including review by the authors wherever possible. If you identify any issues, please contact us.

Publisher's note

All claims expressed in this article are solely those of the authors and do not necessarily represent those of their affiliated

organizations, or those of the publisher, the editors and the reviewers. Any product that may be evaluated in this article, or claim that may be made by its manufacturer, is not guaranteed or endorsed by the publisher.

References

Armijo, R., Tapponnier, P., and Han, T. L. (1989). Late Cenozoic right-lateral strike-slip faulting in southern Tibet. *J. Geophys. Res.* 94 (B3), 2787–2838. doi:10.1029/JB094iB03p02787

Burchfiel, B. C., and Chen, Z. L. (2012). Tectonics of the southeastern Tibetan Plateau and its adjacent foreland. *Mem. Geol. Soc. Am.* 210, 1–164. doi:10.1130/MEM210

Cao, K., Tian, Y. T., van der Beek, P., Wang, G. C., Shen, T. Y., Reiners, P., et al. (2022). Southwestward growth of plateau surfaces in eastern Tibet. *Earth-Science Rev.* 232, 104160. doi:10.1016/j.earscirev.2022.104160

Chayu and Dangxiong earthquake investigation teams in Xizang (1987). Investigation of the 1921 yanjing earthquake in mangkang county (in Chinese with English abstract). *Earthq. Res. Sichuan* 1, 16–17.

Cui, P., Ge, Y. G., Li, S. J., Li, Z. H., Xu, X. W., Gordon, G. D., et al. (2022). Scientific challenges in disaster risk reduction for the Sichuan-Tibet Railway. *Eng. Geol.* 309, 106837. doi:10.1016/j.enggeo.2022.106837

Department of Earthquake Disaster Prevention State Seismological Bureau (1995). *Historical strong earthquake catalog of China (2300 BC-1911 AD)*. Beijing: Seismological Publishing Press, 1–514. (in Chinese).

Ding, L., and Zhong, D. L. (2013). The tectonic evolution of the eastern Himalayas syntaxis since the collision of the Indian and Eurasian plates (in Chinese with English abstract). *Chin. J. Geol.* 48 (2), 317–333. doi:10.3969/j.issn.0563-5020.2013.02.001

Duan, J. Z., and Tan, X. H. (2000). The nature and feature of Cenozoic main strike-slip fault in the Three-River Area of west Yunnan (in Chinese with English abstract). *Yunnan Geol.* 19 (1), 8–23.

Guynn, J. H., Kapp, P., Pullen, A., Heizler, M., Gehrels, G., and Ding, L. (2006). Tibetan basement rocks near Amdo reveal "missing" Mesozoic tectonism along the Bangong suture, central Tibet. *Geology* 34 (6), 505–508. doi:10.1130/G22453.1

Han, M. M., Chen, L. C., Li, Y. B., Gao, S. P., and Feng, J. H. (2022a). Geological and geomorphic evidence for late Quaternary activity of the Bianba-Luolong fault on the western boundary of the Bangong-Nujiang suture (in Chinese with English abstract). *Earth Sci.* 47 (3), 757–765. doi:10.3799/dqkx.2022.042

Han, M. M., Chen, L. C., Li, Y. B., Gao, S. P., and Feng, J. H. (2022b). Paleoearthquakes of the Yangda-Yaxu fault across the Nujiang suture and Lancang river suture zone, southeastern Tibetan Plateau. *Front. Earth Sci.* 10, 990187. doi:10.3389/feart.2022.990187

Heidbach, O., Rajabi, M., Cui, X. F., Fuchs, K., Muller, B., Reinecker, J., et al. (2018). The world stress map database release 2016: crustal stress pattern across scales. *Tectonophysics* 744, 484–498. doi:10.1016/j.tecto.2018.07.007

Kan, R. J., Wang, S. J., Huang, K., and Song, W. (1983). Modern tectonic stress field and relative motion of intraplate block in southwestern China (in Chinese with English abstract). *Seismol. Geol.* 5 (2), 79–90.

Li, M. (2019). Study on the activity of Bangda fault in eastern Tibet and its engineering significance (in Chinese with English abstract). Master's thesis. Chengdu (China): Chengdu University of Technology, 1–84.

Li, S., Yin, C. Q., Guilmette, C., Ding, L., and Zhang, J. (2019). Birth and demise of the bangong-Nujiang Tethyan ocean: a review from the Gerze area of central Tibet. *Earth-Science Rev.* 198, 102907. doi:10.1016/j.earscirev.2019.102907

Li, Y. J., Liu, M., Li, Y. H., and Chen, L. W. (2019). Active crustal deformation in southeastern Tibetan Plateau: the kinematics and dynamics. *Earth Planet. Sci. Lett.* 523, 115708. doi:10.1016/j.epsl.2019.07.010

Li, Z. J., Wang, Y., Gan, W. J., Fang, L. H., Zhou, R. J., Seagren, E. G., et al. (2020). Diffuse deformation in the SE Tibetan Plateau: new insights from geodetic observations. *J. Geophys. Res. Solid Earth* 125, e2020JB019383. doi:10.1029/2020JB019383

Li, H. B., Pan, J. W., Sun, Z. M., Si, J. L., Pei, J. L., Liu, D. L., et al. (2021). Continental tectonic deformation and seismic activity: a case study from the Tibetan Plateau. *Acta Geol. Sin.* 95 (1), 194–213. doi:10.19762/j.cnki.dizhixuebao.2021051

Li, W. Q., Yu, C. Q., Zou, C. C., and Zeng, X. Z. (2023). Three-dimensional density distribution and earthquake activity of the northern Lancangjiang fault in eastern Tibet. *Tectonophysics* 857, 229864. doi:10.1016/j.tecto.2023.229864

Li, C., Zhao, Z. B., Chevalier, M. L., Zheng, Y., Liu, D. L., Lu, H. J., et al. (2024). Lancang fault assists block extrusion in southeastern Tibet during Early-Middle Miocene. *Tectonics* 43, e2024TC008341. doi:10.1029/2024TC008341

Liang, M. J., Luo, N. F., Dong, Y. X., Tan, L., Su, J. R., and Wu, W. W. (2025). Holocene activity characteristics and seismic risk of major earthquakes in the middle segment of the Jinshajiang fault zone, east of the Qinghai-Tibetan Plateau. *Appl. Sci.* 15, 9. doi:10.3390/app15010009

Liu, C. S. (1991). The Yanjing M = 6 earthquake on Dec. 22, 1920 in Mongkang County, Tibet (in Chinese with English abstract). *Earthq. Res. Sichuan* 4, 52–55.

Liu-Zeng, J., Zhang, J. Y., McPhillips, D., Reiners, P., Wang, W., Pik, R., et al. (2018). Multiple episodes of fast exhumation since Cretaceous in southeast Tibet, revealed by low-temperature thermochronology. *Earth Planet. Sci. Lett.* 490, 62–76. doi:10.1016/j.epsl.2018.03.011

Lu, C. F., and Cai, C. X. (2019). Challenges and countermeasures for construction safety during the Sichuan-Tibet Railway Project. *Engineering* 5 (5), 833–838. doi:10.1016/j.eng.2019.06.007

Mao, Y. P., Wang, Y. L., and Li, C. C. (2004). Study on the seismogeological background of dam-induced earthquake of major dam along the middle segment of Lancang River (in Chinese with English abstract). *J. Seismol. Res.* 27 (Suppl. l), 63–69. doi:10.3969/j.issn.1000-0666.2004.z1.013

Metcalfe, I. (2006). Palaeozoic and Mesozoic tectonic evolution and palaeogeography of East Asian crustal fragments: the Korean Peninsula in context. *Gondwana Res.* 9, 24–46. doi:10.1016/j.gr.2005.04.002

Pan, G. T., Wang, L. Q., Li, R. S., Yuan, S. H., Ji, W. H., Yin, F. G., et al. (2012). Tectonic evolution of the Qinghai-Tibet plateau. *J. Asian Earth Sci.* 53, 3–14. doi:10.1016/j.jseaes.2011.12.018

Pan, G. T., Ren, F., Yin, F. G., Wang, L. Q., Wang, B. D., Wang, D. B., et al. (2020). Key zones of oceanic plate geology and Sichuan-Tibet Railway Project (in Chinese with English abstract). *Earth Sci.* 45 (7), 2293–2304. doi:10.3799/dqkx.2020.070

Pei, Q. M., Wang, Hu., Lin, B., Senapathi, V., and Li, D. (2023). Editorial: Sichuan-Tibet traffic corridor: fundamental geological investigations and resource endowment. *Front. Earth Sci.* 11, 1204067. doi:10.3389/feart.2023.1204067

Ren, J. J., Xu, X. W., Lv, Y. W., Wang, Q. X., Li, A., Li, K., et al. (2022). Late Quaternary slip rate of the northern Lancangjiang fault zone in eastern Tibet: seismic hazards for the Sichuan-Tibet Railway and regional tectonic implications. *Eng. Geol.* 306, 106748. doi:10.1016/j.enggeo.2022.106748

Replumaz, A., and Tapponnier, P. (2003). Reconstruction of the deformed collision zone between India and Asia by backward motion of lithospheric blocks. *J. Geophys. Res. Solid Earth* 108 (B6), 2001JB000661. doi:10.1029/2001JB000661

Science and Technology Committee of the Tibetan Autonomous Region (in Chinese) (1982). *Records of historical earthquakes of Tibet*. Lhasa: People's Press of the Tibet.

Shen, J., Wang, Y. P., Ren, J. W., and Cao, Z. Q. (2003). Quaternary dextral shearing and crustal movement in southeast Tibetan Plateau (in Chinese with English abstract). *Xinjiang Geol.* 21 (1), 120–125.

Shen, X. M., Tian, Y. T., Wang, Y., Wu, L., Jia, Y. Y., Tang, X. D., et al. (2021). Enhanced Quaternary exhumation in the central three Rivers region, southeastern Tibet. *Front. Earth Sci.* 9, 741491. doi:10.3389/feart.2021.741491

Shi, S. (2021). Study on fault activity of Changdu-Yanjing segment of Lancang River fault zone (in Chinese with English abstract). Master's thesis. Chengdu (China): Chengdu University of Technology, 1–82.

Tapponnier, P., Xu, Z. Q., Roger, F., Meyer, B., Arnaud, N., Wittlinger, G., et al. (2001). Oblique stepwise rise and growth of the Tibet Plateau. *Science* 294 (5547), 1671–1677. doi:10.1126/science.105978

Taylor, M., Yin, A., Ryerson, F. J., Kapp, P., and Ding, L. (2003). Conjugate strike-slip faulting along the Bangong-Nujiang suture zone accommodates coeval east-west extension and north-south shortening in the interior of the Tibetan Plateau. *Tectonics* 22 (4), 2002TC001361. doi:10.1029/2002TC001361

Wang, M., and Shen, Z. K. (2020). Present-day crustal deformation of continental China derived from GPS and its tectonic implications. *J. Geophys. Res. Solid Earth* 125, e2019JB018774. doi:10.1029/2019JB018774

Wang, G. Z., Hu, R. Z., Fang, W. X., and Tao, X. F. (2001). Strike-slip deformation in Lancang River fault zone and relationship with Ge ore deposit in Lincang, Yunnan (in Chinese with English abstract). *Acta Mineral. Sin.* 21 (4), 695–698. doi:10.3321/j.issn:1000-4734.2001.04.021

Wang, S. J., Qin, J. Z., Li, Z. H., and Long, X. F. (2007). Relationship between seismicity and environmental shear stress field along Lancangjiang fault zone (in Chinese with English abstract). *J. Seismol. Res.* 30 (2), 127–132. doi:10.3969/j.issn.1000-0666.2007.02.004

Wang, X. Z., Qiangba, Z. X., and Peng, X. J. (2008). A discussion about the geological nature of Lancangjiang fault zone in east Xizang-west Yunnan (in Chinese with English abstract). *Yunnan Geol.* 27 (3), 362–370. doi:10.3969/j.issn.1004-1885.2008.03.014

Xia, J. W., and Zhu, M. (2020). Study on tectonic characteristics and activity of middle section of Jinshajiang main fault zone (in Chinese with English abstract). *Yangtze River* 51 (5), 131–137.

Xu, Z. H., Wang, S. Y., Huang, Y. R., Gao, A. J., Jin, X. F., and Chang, X. D. (1987). Directions of mean stress axes in southwestern China deduced from microearthquake data (in Chinese with English abstract). *Acta Geophys. Sin.* 30 (5), 476–486.

Yin, A., and Harrison, T. M. (2000). Geologic evolution of the Himalayan-Tibetan orogen. *Annu. Rev. Earth Planet. Sci.* 28, 211–280. doi:10.1146/annurev.earth.28.1.211

Yu, W. X., An, X. W., Li, S. C., Zhou, R. Q., and Yang, J. W. (2002). Study on SEM characteristics of quartz grains in the fault gouges of the main faults and the fault activity in the Lancang River valley (in Chinese with English abstract). *J. Seismol. Res.* 25 (3), 275–280. doi:10.3969/j.issn.1000-0666.2002.03.012

Zhang, B., Zhang, J. J., Zhong, D. L., and Guo, L. (2009). Architecture, kinematics and thermochronology analysis in Lancangjiang Structural Zone, in western Yunnan (in Chinese with English abstract). *Chin. J. Geol.* 44 (3), 889–909. doi:10.3321/j.issn:0563-5020.2009.03.009

Zhang, K. J., Zhang, Y. X., Tang, X. C., and Xia, B. (2012). Late Mesozoic tectonic evolution and growth of the Tibetan plateau prior to the Indo-Asian collision. *Earth-Science Rev.* 114, 236–249. doi:10.1016/j.earscirev.2012.06.001

Zhang, D., Hu, C. Z., Tian, Q. J., Yang, P. X., Liang, P., Cui, T. F., et al. (2022). Study on geometric distribution and activity characteristics of Naozhong fault based on Gaofen-7 stereo pair and UAV aerial survey images (in Chinese with English abstract). *Seismol. Geomagnetic Observation Res.* 43 (Suppl. 11), 79–82. doi:10.3969/j.issn.1003-3246.2022.S1.026

Zhang, P. Z., Wang, W. T., Gan, W. J., Zhang, Z. Q., Zhang, H. P., Zheng, D. W., et al. (2022). Present-day deformation and geodynamic processes of the Tibetan Plateau. *Acta Geol. Sin.* 96 (10), 3297–3313. doi:10.19762/j.cnki.dizhixuebao.2022295

Zhang, X. B., Yu, H., Yu, X., Guo, C. B., Wu, R. A., Wang, Y., et al. (2024). Preliminary study on the late Quaternary activity of important active fault zones along the Yunnan-Tibet Railway (in Chinese with English abstract). *Prog. Earthq. Sci.* 54 (1), 94–109. doi:10.19987/j.dzkxjz.2023-147

Zhong, K. H., Liu, Z. C., Shu, L. S., Li, F. Y., and Shi, Y. S. (2004). The Cenozoic strike-slip kinematics of the Lancangjiang fault zone (in Chinese with English abstract). *Geol. Rev.* 50 (1), 1–8. doi:10.3321/j.issn:0371-5736.2004.01.001

Zhong, N., Yang, Z., Zhang, X. B., Ding, Y. Y., Wu, R. A., Wang, Y., et al. (2022). Evidence of Holocene activity and paleoseismic records in the central section of Bangda fault in Nujiang fault zone (in Chinese with English abstract). *Geol. Rev.* 68 (6), 2021–2032. doi:10.16509/j.georeview.2022.08.131